ChemComm

COMMUNICATION

View Article Online
View Journal | View Issue

Cite this: *Chem. Commun.*, 2022, **58**, 8262

Received 20th June 2022,
Accepted 27th June 2022

DOI: 10.1039/d2cc03409c

rsc.li/chemcomm

Polymerization-like mechanism for fixation of CO_2 with epoxides by multifunctional organocatalysts†

Mingan Chen, Hui Yang and Ming Wah Wong *

The commonly accepted mechanism of CO_2 fixation of epoxides to cyclic carbonates catalyzed by multifunctional non-halide organocatalysts is challenged by our computational DFT-D3 study, which revealed a new polymerization-like mechanism comprising alternate epoxide and CO_2 activation steps and a nested CO_2 activation pathway. We investigated a recently reported CO_2 coupling with epoxide reaction catalyzed by a bis-phenolic multifunctional catalyst. The predicted *cis*/*trans* product ratio is in excellent agreement with experimental results. The general applicability of the new mechanism is supported by another diamine-diacid catalyzed CO_2 fixation reaction.

CO_2 fixation with epoxides to synthesize cyclic carbonates represents one of the successful strategies to utilize the greenhouse gas. In the wake of the harm to the environment, there has been a growing interest in developing efficient organocatalysts for the chemical fixation processes of industrial feedstock, particularly the green halide-free catalysts.[1–3] One of the major challenges in catalyst design is the lack of thorough understanding of the mechanism of activation, which holds the key to further catalyst activity improvement. Although many multifunctional halide-free organocatalysts have recently been reported,[1–11] not much progress has been made in the in-depth understanding of the catalytic mechanism.

Three mechanisms are commonly proposed for CO_2 fixation with epoxides, namely epoxide activation, CO_2 activation and dual activation (Scheme 1). The first is the most commonly proposed one, with experimental and computational support.[2] In this pathway, the catalysts act as Lewis or Brønsted acids to activate the oxygen atoms of epoxides, which makes them more susceptible to nucleophilic ring opening. The nucleophiles are usually halides but are increasingly replaced by other nucleophilic groups, such as onium salts, hydrogen bond donors and tertiary amines, which are either a part of the acid catalysts or added separately. The second CO_2 activation mechanism involves nucleophilic activation of CO_2 in the first step, generating reactive carboxylate intermediates that open the epoxides. It requires the catalyst to be nucleophilic towards CO_2, but not towards epoxides. For the dual activation mechanism, with simultaneous activation of CO_2 and epoxides, it involves an initial nucleophilic addition of the catalysts to CO_2 instead of to the epoxides (Scheme 1).

To date, the majority of computational studies in the literature support the epoxide activation mechanism.[12–15] However, proposals of CO_2 activation and dual activation mechanisms have increased substantially in recent reports on halide-free multifunctional organocatalyzed CO_2 fixation.[4,7,10,16,17] One major supporting evidence for such proposals is the experimental detection and sometimes isolation of catalyst-CO_2 adducts, although scarcely any computational studies have confirmed the CO_2 activation pathway in such cases. For example, a DFT study on NHC-catalyzed CO_2 fixation found that the earlier-proposed CO_2 activation mechanism is less favorable and the catalysis is likely to follow the epoxide activation mechanism.[12] In fact, it is likely that the catalyst-CO_2 adducts may just be a resting state of the catalyst, and the cycloaddition reaction follows a different mechanism.[6]

Another important piece of supporting evidence for the CO_2 activation pathway comes from studies of the stereochemistry of deuterated products of terminal epoxides. Young *et al.* proposed that the epoxide activation mechanism involves two S_N2 reactions at the same carbon (bound to R^1 in species **a** and **c**, Scheme 1), resulting in a retention of stereochemistry in the products.[18] In contrast, the CO_2 activation pathway involves only one S_N2 reaction (between **e** and **f**), which leads to an inversion of the product stereochemistry. One excellent example is the recent work by North and co-workers, who reported salophen *N*,*N*′-phenylenebis(5-*tert*-butylsalicylideneimine) **1**-catalyzed cycloaddition of CO_2 with epoxides.[8] Their stereochemical study revealed that *trans*-epoxide **2a** yields almost equal amounts of *trans*- and *cis*-products (Scheme 2),

Department of Chemistry, National University of Singapore, 3 Science Drive 3, 117543, Singapore. E-mail: chmwmw@nus.edu.sg

† Electronic supplementary information (ESI) available: Detailed computational results, total energies and Cartesian coordinates of all calculated structures; choice of DFT method and solvent; comparison with computational work of Jiao *et al.*; other mechanistic pathways. See DOI: https://doi.org/10.1039/d2cc03409c

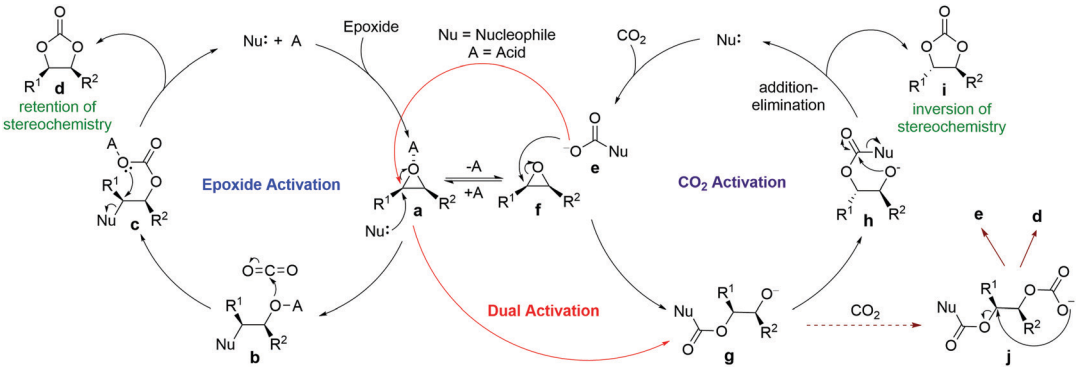

Scheme 1 Generally proposed reaction mechanisms of organocatalyzed CO_2 fixation.

which suggests that both the epoxide and CO_2 activation mechanisms are in operation. A novel bi-CO_2 activation mechanism was proposed to explain the uncommon stereochemistry result, which involves another CO_2 activation after intermediate **g** to form **j** in Scheme 1, yielding product **d** with retention of stereochemistry.[8] Interestingly, a recent computational study of this reaction by Jiao and co-workers concluded that the epoxide activation mechanism is still favored over the CO_2 activation mechanism.[19] However, the authors failed to rationalize the distribution of product stereochemistry based on their proposed epoxide activation mechanism. The inconsistency in activation pathway and product stereochemistry distribution between theory and experiment undermines the confidence in the currently proposed mechanisms and a thorough computational mechanistic study is warranted.

Previous mechanistic proposals hypothesized that the catalytic cycle initiates either through activating the epoxide substrate or CO_2 by the catalyst, followed by nucleophilic reaction with the other substrate. To better understand the intriguing stereochemistry results, we first re-examined both mechanisms of **1**-catalyzed CO_2 fixation with epichlorohydrin (**2b**) using M06-2X[20] theory with D3[21] dispersion correction in the solution phase with the SMD[22] solvation model (see ESI† for rationales for the DFT method and solvent choices). Transition state (TS) conformation sampling was carried out using our recently developed docking program QMTSDock[23] at the Hartree–Fock level. The low-energy conformers obtained from docking were subjected to further optimization at the DFT level. Several important improvements on the key TS structures were obtained, with significantly lower activation barriers for the CO_2 activation pathway compared to those reported by Jiao *et al* (see ESI† for detailed discussion). The results are summarized in Scheme 3. In addition to comparing various activation modes, we also compared the two possible nucleophilic sites of catalyst **1**, namely the hydroxyl and imine groups, and calculated their reactivities towards the epoxide electrophile. Our calculations showed that the hydroxyl group is a better nucleophile when the imine serves as a Brønsted base to deprotonate it (see ESI† for the pathway utilizing the imine group as the nucleophile). The second hydroxyl group is essential for a low activation barrier, *via* transferring a proton to the developing oxyanion in the transition state **TS-A-1** (Fig. 1). In agreement with the computational study by Jiao *et al.*, the epoxide activation pathway still has a significantly lower activation barrier than that of the CO_2 activation pathway (46.6 *vs.* 57.6 kcal mol^{-1}). In other words, the observed product stereochemistry distribution cannot be explained by the conventional CO_2 activation pathway catalyzed by **1**.

To find an alternative mechanism that explains the inversion product, it is instructive to gain a deeper understanding of the conventional CO_2 mechanism first. One major hypothesis of CO_2 activation is that the generated CO_2 adduct that has a formal charge separation is a more potent nucleophile to epoxide addition than the original catalyst. Indeed, our calculated result is consistent with this hypothesis. The barrier for adding CO_2-catalyst adduct **INT-B-1** to epoxide through **TS-B-2** is 39.2 kcal mol^{-1}, 7.4 kcal mol^{-1} lower than that of **TS-A-1** in the epoxide activation mechanism. However, addition of catalyst **1** to CO_2 is highly unfavorable, with product **INT-B-1** being 18.4 kcal mol^{-1} higher in energy. In other words, although adduct **INT-B-1** is a better nucleophile than catalyst **1**, it is thermodynamically unfavorable to form in the first place.

We noticed that in the epoxide activation mechanism, intermediate **INT-A-1** also adds to CO_2 but yields adduct **INT-A-2** that is more favorable energetically, only 13.7 kcal mol^{-1} higher. Based on these findings, we envisage that imino alcohol **INT-A-1** could be a better catalyst than **1** to promote CO_2 activation, yielding the inversion product **P-I**. In this case, the CO_2 activation cycle catalyzed by **INT-A-1** would be nested inside the conventional epoxide activation cycle, sharing the CO_2 addition step from **INT-A-1** to **INT-A-2** (Scheme 3) with it.

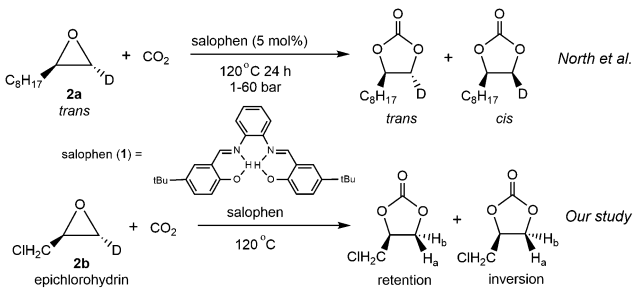

Scheme 2 Stereochemistry studies with salophen catalyst **1**.

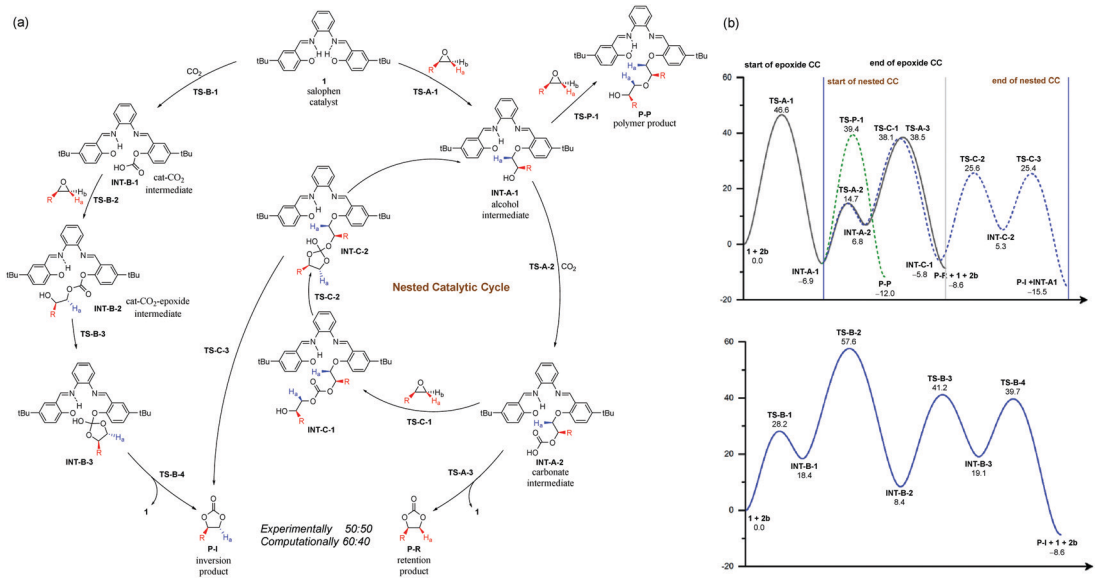

Scheme 3 (a) Explored reaction pathways with a nested catalytic cycle (CC), (b) (top) calculated reaction profiles with initial activation of the epoxide substrate and (bottom) calculated reaction profile for the conventional CO_2 activation mechanism. R = CH_2Cl and relative free energies are in kcal mol^{-1}. Proton transfer reactions are omitted for clarity.

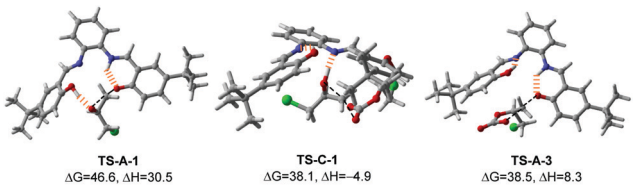

Fig. 1 Optimized geometries of key transition states (activation barriers in kcal mol^{-1}). Hydrogen bonds are shown as hashed lines.

The two cycles diverge from **INT-A-2** and thus the product stereochemistry distribution would depend on the relative energies of **TS-C-1** *versus* **TS-A-3**. Recognizing the similarity between the two TSs, both belonging to an S_N2 reaction at a carbon center with an oxygen atom leaving group and the ring strain of the epoxide molecule, we hypothesize that the product stereochemistry could be rationalized by comparing the newly proposed nested CO_2 activation pathway and the conventional epoxide activation pathway. A similar mechanism leading to polymeric carbonates is well known in metal-catalyzed CO_2-fixation reactions with epoxides.[24,25] However, it has not been proposed or studied computationally in organocatalyzed reactions, probably due to the preconception that a metal center is needed to sustain polymeric chain growth.

The calculated reaction profile of the nested CO_2 activation pathway is shown in Scheme 3 and the optimized key TSs are shown in Fig. 1. The two TSs responsible for product stereochemistry distribution, namely **TS-C-1** and **TS-A-3**, are indeed close in energy, with a $\Delta\Delta G^{\ddagger}$ difference of just 0.4 kcal mol^{-1} in favor of the former. This is in good agreement with the observed almost equal yields of the inversion (**P-I**) and retention (**P-R**) products. The predicted small energy difference between the two stereoselective TSs is confirmed by higher level computational theories, namely double-hybrid DFT and DLPNO-CCSD(T) methods (see ESI† for benchmarking details). The calculated overall barriers are somewhat high compared to the experimental conditions. These slightly higher values are likely due to the systematic error of the DFT method (see ESI† for benchmark detail). Although **TS-C-1** is entropically less favorable than **TS-A-3** due to addition to another molecule from **INT-A-2**, it is 13.2 kcal mol^{-1} lower in enthalpy, which offsets the entropic disadvantage. Unlike **TS-A-1** that prefers the simultaneous assistance of two hydrogen bonds, **TS-C-1** and **TS-A-3** prefer only one hydrogen bond assistance to the substrate (Fig. 1). It is important to note that the hydrogen bonding of the imine groups plays a crucial role of proton transfer in the catalytic mechanism (see ESI† for detailed examples).

Although the nested catalytic cycle in Scheme 3 gives an excellent explanation of the product stereochemistry, it is natural to ask if a polymeric carbonate pathway as in metal-catalyzed reactions[24] would lead to polymer formation here. To this end, we investigated the pathways of adding one and two more repeating units, CO_2 and then epichlorohydrin in that order, to **INT-C-1** (see ESI† for more detail). The computational result showed that further polymer growth is increasingly difficult, possibly due to the small size of catalyst **1**, which makes it increasingly entropically unfavorable to stabilize the growing polymer chain through a hydrogen bond from the imine group. Besides, the epoxides are being added away from the catalytic system, in contrast to the insertion from a typical metal center (initiator). Another pathway leading to polyether formation was also investigated and the associated transition state **TS-P-1** was found to be 1.3 kcal mol^{-1} higher than **TS-C-1** (Scheme 3). The closeness of the reaction barriers between the

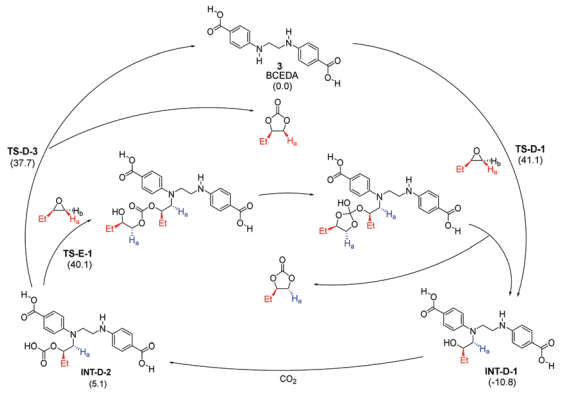

Scheme 4 Calculated mechanism of multifunctional BCEDA-catalyzed CO_2 fixation with 1,2-epoxybutane. Relative free energies in kcal mol^{-1}.

polymer and cyclic carbonate pathways makes it hard to exclude the former confidently. It is likely that minor polymer products are formed together with the major cyclic carbonate product. In other words, the proposed mechanism is only polymerization-like but without significant polymer formation. This may explain why the observed yield of cyclic carbonate is about 8% lower than the total conversion.[8] It is worth noting that the cyclic carbonate can be formed by a backbiting mechanism from a growing polymer chain.[26] However, this alternative pathway is unlikely due to increasing difficulty in the polymer growth (see ESI†).

One key feature of the new mechanism is the organocatalytic cascade leading to the formation of the stereochemically inverted *trans* product through the CO_2 activation pathway catalyzed by a reactive intermediate, namely **INT-A-1**. The second key feature is that the proposed CO_2 and epoxide activation pathways are both an integral part of a polymerization-like pathway, differing in their exit points. It seems clear that the two activation pathways are not locked in an either-or relationship, but rather a stereochemically complementary and mechanistically integrated one. With the ongoing development of more efficient multifunctional organocatalysts, we expect to see more such examples. Due attention should be paid to leverage this complementary and integrated relationship, whether to understand the mechanism or design new catalysts. To demonstrate the general applicability of this polymerization-like mechanism, we chose to study another recently reported reaction catalyzed by a multifunctional diamine-diacid catalyst BCEDA (short for *N*,*N*′-bis(4-carboxyphenyl)ethylenediamine).[11] Our preliminary theoretical investigation, based on the same M06-2X-D3 theory (Scheme 4), suggests that the difference between the nested CO_2 activation pathway and the epoxide activation pathway is only 2.4 kcal mol^{-1} (difference between **TS-D-3** and **TS-E-1**). In contrast, the conventional CO_2 activation mechanism proposed by the authors is ~15 kcal mol^{-1} higher in energy than the epoxide pathway.

In summary, we have shown through comprehensive computational investigation that along with the conventional epoxide activation pathway, a simultaneous polymerization-like mechanism can be in operation during the salophen-catalyzed CO_2 coupling with epoxides. The proposed new mechanism comprises a nested CO_2 activation pathway that is catalyzed by an alcohol intermediate. The predicted *cis*/*trans* product ratio of 40 : 60 (see ESI† for detailed calculations) is in excellent agreement with the experimental finding. This is the first time that the CO_2 activation pathway has been demonstrated computationally to be competitive to the epoxide pathway in organocatalyzed CO_2 fixation with epoxide. The applicability of the new polymerization-like mechanism was confirmed by studying another organocatalyzed CO_2 fixation reaction. We believe that the new computational insights of the relationship between the two mechanisms will lead to better understanding of the experimental results and designing of more efficient multifunctional organocatalysts for CO_2 fixation.[27]

This research was supported by Singapore Ministry of Education (Grant no: A-008483-00-00).

Conflicts of interest

The authors declare no conflicts of interest.

Notes and references

1 M. Alves, B. Grignard, R. Mereau, C. Jerome, T. Tassaing and C. Detrembleur, *Catal. Sci. Tech.*, 2017, **7**, 2651–2684.
2 L. P. Guo, K. J. Lamb and M. North, *Green Chem.*, 2021, **23**, 77–118.
3 F. Zhang, Y. Wang, X. Zhang, X. Zhang, H. Liu and B. Han, *Green Chem. Eng.*, 2020, **1**, 82–93.
4 P. Goodrich, H. Q. N. Gunaratne, J. Jacquemin, L. Jin, Y. Lei and K. R. Seddon, *ACS Sustainable Chem. Eng.*, 2017, **5**, 5635–5641.
5 L. Guglielmero, A. Mezzetta, C. S. Pomelli, C. Chiappe and L. Guazzelli, *J. CO2 Util.*, 2019, **34**, 437–445.
6 A.-H. Liu, Y.-L. Dang, H. Zhou, J.-J. Zhang and X.-B. Lu, *ChemCatChem*, 2018, **10**, 2686–2692.
7 A. A. Pawar and H. Kim, *J. CO2 Util.*, 2019, **33**, 500–512.
8 X. Wu, C. Chen, Z. Guo, M. North and A. C. Whitwood, *ACS Catal.*, 2019, **9**, 1895–1906.
9 S. Yue, X.-J. Hao, P.-P. Wang and J. Li, *Mol. Catal.*, 2017, **433**, 420–429.
10 Z. Yue, M. Pudukudy, S. Chen, Y. Liu, W. Zhao, J. Wang, S. Shan and Q. Jia, *Appl. Catal., A*, 2020, **601**, 117646.
11 F. Zhang, S. Bulut, X. J. Shen, M. H. Dong, Y. Y. Wang, X. M. Cheng, H. Z. Liu and B. X. Han, *Green Chem.*, 2021, **23**, 1147–1153.
12 M. J. Ajitha and C. H. Suresh, *Tetrahedron Lett.*, 2011, **52**, 5403–5406.
13 H.-G. Kim, C.-S. Lim, D.-W. Kim, D.-H. Cho, D.-K. Lee and J. S. Chung, *Mol. Catal.*, 2017, **438**, 121–129.
14 W. Natongchai, J. A. Luque-Urrutia, C. Phungpanya, M. Solà, V. D'Elia, A. Poater and H. Zipse, *Org. Chem. Front.*, 2021, **8**, 613–627.
15 S. Ryu, *Bull. Korean Chem. Soc.*, 2019, **40**, 1033–1038.
16 J. A. Kozak, J. Wu, X. Su, F. Simeon, T. A. Hatton and T. F. Jamison, *J. Am. Chem. Soc.*, 2013, **135**, 18497–18501.
17 G. Yuan, Y. Zhao, Y. Wu, R. Li, Y. Chen, D. Xu and Z. Liu, *Sci. China Chem.*, 2017, **60**, 958–963.
18 C. Beattie, M. North, P. Villuendas and C. Young, *J. Org. Chem.*, 2013, **78**, 419–426.
19 C.-H. Guo, M. Liang and H. Jiao, *Catal. Sci. Tech.*, 2021, **11**, 2529–2539.
20 Y. Zhao and D. G. Truhlar, *Theor. Chem. Acc.*, 2008, **120**, 215–241.
21 S. Grimme, J. Antony, S. Ehrlich and H. Krieg, *J. Chem. Phys.*, 2010, **132**, 154104.
22 A. V. Marenich, C. J. Cramer and D. G. Truhlar, *J. Phys. Chem. B*, 2009, **113**, 6378–6396.
23 H. Yang and M. W. Wong, *J. Phys. Chem. A*, 2019, **123**, 10303–10314.
24 A. J. Kamphuis, F. Picchioni and P. P. Pescarmona, *Green Chem.*, 2019, **21**, 406–448.
25 A. Brege, B. Grignard, R. Méreau, C. Detrembleur, C. Jerome and T. Tassaing, *Catalysts*, 2022, **12**, 124.
26 M. Taherimehr, S. M. Al-Amsyar, C. J. Whiteoak, A. W. Kleij and P. P. Pescarmona, *Green Chem.*, 2013, **15**, 3083–3090.
27 N. Liu, Y.-F. Xie, C. Wang, S.-J. Li, D. Wei, M. Li and B. Dai, *ACS Catal.*, 2018, **8**, 9945–9957.